

NACA TN 3617

2066

9-83

TECH LIBRARY KAFB, NM  
0066438

# NATIONAL ADVISORY COMMITTEE FOR AERONAUTICS

TECHNICAL NOTE 3617

THEORETICAL ANALYSIS OF LINKED LEADING-EDGE AND  
TRAILING-EDGE FLAP-TYPE CONTROLS

AT SUPERSONIC SPEEDS

By E. Carson Yates, Jr.

Langley Aeronautical Laboratory  
Langley Field, Va.



Washington

March 1956

AFMDC  
TECHNICAL LIBRARY



## TECHNICAL NOTE 3617

## THEORETICAL ANALYSIS OF LINKED LEADING-EDGE AND

## TRAILING-EDGE FLAP-TYPE CONTROLS

## AT SUPERSONIC SPEEDS

By E. Carson Yates, Jr.

## SUMMARY

The use of linked leading-edge and trailing-edge flap-type controls for the purpose of reducing hinge moments at supersonic speeds has been analytically investigated. A series of linked controls with supersonic leading and trailing edges on swept and unswept wings has been studied for Mach numbers of 1.414 and 1.960 by use of the linearized theory of supersonic flows. Variations of lift, rolling moment, and hinge moment with control deflection for these control combinations have been calculated, and the effect of finite wing thickness on these quantities has been estimated. Control characteristics have been tabulated for the condition of equal leading-edge and trailing-edge flap deflection, and the deflection ratios necessary for zero resultant hinge moment have also been listed.

## INTRODUCTION

The problem of reducing the excessive hinge moments which accompany deflection of flap-type controls at supersonic speeds has not yet been satisfactorily solved. Available theoretical information (ref. 1) can be used to estimate for a given wing or tail the flap-type controls yielding minimum hinge moments due to deflection for a given rolling moment or lift, but the need for a method of reducing hinge moments and stick forces still exists. One possible solution to the problem may be obtained by mechanically linking a leading-edge flap and a trailing-edge flap so that the hinge moment of one cancels part or all of the hinge moment of the other while both produce lift or rolling moment or both. A control arrangement of this kind may also yield reduced pitching moments and hence a reduction in the tendency toward wing twist and aileron reversal. An early theoretical investigation of two-dimensional linked leading- and trailing-edge flaps by means of linearized subsonic flow theory has been given in reference 2. Reference 3 contains results of some two-dimensional subsonic tests. Some supersonic tests have been made on three-dimensional configurations (see, for example, refs. 4, 5, and 6), but these experiments were very limited in scope and the results are far from conclusive.

The desirability of the linked-flap control system would depend primarily on the following factors:

- (1) The ability of the system to cancel a large portion of the hinge moment by use of reasonably small deflection ratio (ratio of leading-edge flap deflection to trailing-edge flap deflection)
- (2) The variation of system characteristics with Mach number
- (3) The magnitude of nonlinearities in the variation of control characteristics with flap deflection or angle of attack (nonlinearities caused, for example, by interference between the control surfaces by viscous effects, or by detached shocks)

In order to obtain information regarding some of these properties, an analytical investigation has been made to determine the variation of aerodynamic forces and moments with control deflection and Mach number for several flap combinations on two wing plan forms. These configurations include seven combinations of partial-span leading- and trailing-edge controls on an unswept tapered wing at Mach numbers of 1.414 and 1.960 and two combinations of partial-span controls on a 45° sweptback tapered wing at a Mach number of 1.960. The calculations are based on the linearized theory of supersonic flows as presented in references 7 and 8, and the method of reference 8 is used also to estimate the effect of finite wing thickness.

#### SYMBOLS

M free-stream Mach number

$$\beta = \sqrt{M^2 - 1}$$

$\Lambda$  angle of sweep, positive for sweepback

b wing span

$b_f$  flap span

c local wing chord

$c_f$  local flap chord

$\lambda$  taper ratio of wing  $\left(\frac{c_t}{c_r}\right)$

$\lambda_f$  taper ratio of flap  $\left(\frac{c_{f,t}}{c_{f,r}}\right)$

S area of complete wing

$S_f$  area of deflected flap or flaps (on one semispan of wing)

$$S_f = \frac{\beta b_f^2 (a - d) (1 + \lambda_f)}{2(1 - \lambda_f)} = \frac{1}{6} \frac{c_f}{c} \frac{b_f}{b/2} \left(\frac{1}{\lambda_f} + 1\right) \left(\frac{b}{2}\right)^2$$

A aspect ratio of complete wing

$M_a$  area moment of control surface about hinge line

$$M_a = \frac{\beta^2 b_f^3 (a - d)^2 (1 - \lambda_f^3)}{6(1 - \lambda_f)^3 \sqrt{1 + \beta^2 a^2}} = \frac{1}{54} \left(\frac{c_f}{c}\right)^2 \frac{b_f}{b/2} \frac{1 + \lambda_f + \lambda_f^2}{\lambda_f^2} \frac{1}{\sqrt{1 + \beta^2 a^2}} \left(\frac{b}{2}\right)^3$$

$F_1$  thickness correction factor for lift and rolling moment

$F_2$  thickness correction factor for hinge moment

t local airfoil thickness

x streamwise coordinate measured from leading edge rearward

$\delta$  control-surface deflection angle measured in free-stream direction, deg (positive when flap trailing edge is deflected downward relative to flap leading edge)

q free-stream dynamic pressure

$$C_L = \frac{L}{qS/2}$$

$$C_{L,f} = \frac{L}{qS_f}$$

$$C_l = \frac{L'}{qbS/2}$$

$$C_{l,f} = \frac{L'_{PL}}{qb_f S_f}$$

$$C_{m,HL} = \frac{\text{Pitching moment about hinge axis induced by control deflection}}{2qM_a}$$

$$C_h = \frac{H}{2qM_a}$$

L total lift on semispan wing

$L_f$  portion of lift carried by flap or flaps

$L'_{PL}$  rolling moment about control parting line induced by control deflection on semispan wing

$L'_{f,PL}$  rolling moment about control parting line due to  $L_f$

$L'$  total rolling moment about wing-root chord induced by control deflection on semispan wing,  $L'_{PL} + L\left(\frac{b}{2} - b_f\right)$

H hinge moment

$$a = \frac{\tan \Lambda_{HL}}{\beta}$$

$$d = \frac{\tan \Lambda_{TE}}{\beta}$$

$\Delta C_h$  increment of hinge-moment coefficient of trailing-edge flap caused by deflection of leading-edge flap

Subscripts:

LE leading edge

TE trailing edge

$\delta$  partial derivative with respect to control-deflection angle

c/2	midchord line
c/4	quarter-chord line
t	tip
r	root
HL	hinge line
PL	parting line (flap root)

#### FLAP DESIGNATIONS

For convenience, the linked-control configurations are designated by a combination of decimal numbers indicative of the flap dimensions. For configurations with leading- and trailing-edge flaps of equal span, a three-number designation is used, the first number of which represents the quantity  $\frac{b_f}{b/2}$ ; the second,  $\frac{c_{f,LE}}{c}$ ; the third,  $\frac{c_{f,TE}}{c}$ . For configurations with leading- and trailing-edge flaps of unequal span, a four-number designation is used - the first and second numbers representing  $\frac{b_{f,LE}}{b/2}$  and  $\frac{b_{f,TE}}{b/2}$ , respectively, and the third and fourth denoting  $\frac{c_{f,LE}}{c}$  and  $\frac{c_{f,TE}}{c}$ . For example, configurations and their associated dimension ratios are illustrated as follows:

Configuration	$\frac{b_{f,LE}}{b/2}$	$\frac{b_{f,TE}}{b/2}$	$\frac{c_{f,LE}}{c}$	$\frac{c_{f,TE}}{c}$
.50.05.15	0.50	0.50	0.05	0.15
.22, .50.10.15	.22	.50	.10	.15

#### SCOPE AND LIMITATIONS

The investigation is limited to consideration of wings and controls with supersonic leading and trailing edges and streamwise root and tip

chords. The configurations investigated include seven combinations of partial-span leading- and trailing-edge controls on a wing unswept at the midchord line, for which calculations were made at Mach numbers of 1.414 and 1.960, and two combinations of partial-span controls on a wing sweptback  $45^\circ$  at the quarter-chord line, for which calculations were made at a Mach number of 1.960. Both wings have aspect ratios of 4 and taper ratios of 0.5. These configurations are shown in figure 1. All controls considered are located at the wing tip, and the ratio of local control chord to local wing chord for each control is constant along the control span. Reference 1 indicates that the trailing-edge-flap configurations investigated should in themselves yield relatively low hinge moments. The calculations are simplified by choosing configurations such that no Mach line crosses wing or control root or tip chords and such that the wing-tip Mach line does not extend inboard of the trailing-edge flap.

Although this investigation is primarily concerned with lateral-control devices, consideration of the lift properties of the various configurations should give some indication of usefulness as a longitudinal control. However, pitching-moment coefficients for the flap combinations have not been evaluated.

Inasmuch as the present analysis does not constitute an exhaustive investigation, mention should be made of some of the aspects which are not treated. Nonlinearities in the variation of control characteristics with deflection or angle of attack cannot be evaluated by the linearized theory. However, nonlinearities caused by viscosity or detached shocks might not be serious if leading-edge flap deflections are kept small. Unlike the analysis of reference 1, the present work does not indicate an "optimum" configuration, since the net hinge moment depends on the flap deflection ratio  $\delta_{LE}/\delta_{TE}$ . The effect of angle of attack on hinge moment is not determined, since emphasis herein is placed on lateral control. The dynamic effect of time lag (time required for flow to travel from leading-edge flap to trailing-edge flap) is not investigated.

Structural problems are beyond the scope of this paper, but they should not be overlooked in any consideration of this type of control system. The thinness of wings required for supersonic speed will aggravate problems of weight, rigidity of flaps and linkage, and the necessity of changing deflection ratios for satisfactory subsonic performance.

#### THEORETICAL CONSIDERATIONS

Calculations of lift, rolling moment, and hinge moment are based on charts presented in reference 8, which were obtained from the linearized theory of two-dimensional and conical supersonic flows given in reference 7. Also, some unpublished equations obtained in connection with

reference 8 have been used to adapt the results of that investigation for use in determining the interference loads. All equations and details of the calculation procedure are given in appendix A.

Figure 2 shows positive directions of force, moment, and flap deflections, and figure 3 illustrates the superposition of deflections which yields simultaneous deflection of the linked controls according to linearized theory. Figure 3 also shows the Mach lines which separate two-dimensional and conical flow regions.

#### Bases Used in Comparison of Linked

#### Controls - Deflection Ratios

In general, the net hinge moment of the linked system is

$$\frac{H}{2q\delta_{TE}} = \frac{H_{TE \text{ alone}}}{2q\delta_{TE}} + M_{a,TE} \Delta C_{h\delta} \frac{\delta_{LE}}{\delta_{TE}} + \frac{H_{LE}}{2q\delta_{LE}} \frac{d\delta_{LE}}{d\delta_{TE}} \frac{\delta_{LE}}{\delta_{TE}} \quad (1)$$

where the second term on the right represents the increment of trailing-edge-flap hinge moment due to leading-edge-flap deflection, and  $\frac{d\delta_{LE}}{d\delta_{TE}}$  is

the gearing ratio. Most of the calculations for the linked-control configurations are not compared on the basis of  $H = 0$  because, for piloted aircraft, the desirability of maintaining some control feel would make complete cancellation of hinge moments unnecessary. Values of forces and moments for linked and single controls are calculated on the basis of

equal deflection of leading- and trailing-edge controls  $\left(\frac{\delta_{LE}}{\delta_{TE}} = 1\right)$ . In

addition to comparison of the controls on the basis of  $\frac{\delta_{LE}}{\delta_{TE}} = 1$ , equation (1) is solved (see appendix A) for the deflection ratio  $\frac{\delta_{LE}}{\delta_{TE}}$  for

the case of  $H = 0$  with constant gearing ratio. The resulting deflection ratios yield  $H = 0$  for all deflections. Equation (1) is also solved for the deflection ratio for  $H = 0$  with nonconstant gearing ratio. It should be observed that the case of nonconstant gearing ratio is of interest only if the leading- and trailing-edge flaps are connected by a nonlinear linkage. With nonconstant gearing ratio, hinge moment may be completely canceled only at a finite number of deflection conditions.

## Correction for Finite Thickness

In addition to the linearized-theory results, some calculations are made by use of the method of reference 8 to obtain an approximate correction of the linearized-theory results for the effect of finite wing thickness. The correction is applied for a 4-percent-thick symmetrical wedge airfoil section perpendicular to the 0.50c line with  $\left(\frac{t}{c}\right)_{\max}$  at the 0.50c line. Application of this correction is discussed in appendix B.

## PRESENTATION OF RESULTS

Results of the calculations of hinge moment, lift, and rolling moment are presented in table I for trailing-edge flaps deflected singly (columns 2, 3, 6, 8, 10, 12, 14, 16) and in combination with leading-edge flaps. Linked-control hinge-moment, lift, and rolling-moment characteristics are presented for unit deflection ratio  $\left(\frac{\delta_{LE}}{\delta_{TE}} = 1\right)$  (columns 5, 7, 9, 11, 13, 15, 17, 18, 19, 20, 21). In addition, deflection ratios  $\frac{\delta_{LE}}{\delta_{TE}}$  are given for the conditions of zero net hinge moment with constant (column 22) and nonconstant (column 23) gearing ratio. Also presented are results which include corrections for the effect of finite wing thickness (columns 24 to 30).

## DISCUSSION

## Hinge Moment and Hinge-Moment Reduction

Deflection ratio of unity.- Attention is directed to column 19 of table I, where the ratio  $\frac{H_{\text{Linked}}}{H_{\text{TE alone}}}$  is presented for the purpose of comparing the hinge-moment characteristics of the various linked flaps with those of the trailing-edge flaps alone. These comparisons are made on the basis of equal deflection of leading- and trailing-edge flaps.

For leading- and trailing-edge flaps of equal span, the addition of a 0.10c leading-edge flap to the unswept wing with a 0.15c trailing-edge flap (configuration .50.10.15 or .40.10.15) at Mach numbers of 1.414 and 1.960 results in hinge-moment reductions of approximately 0.5. (The quantity  $1 - \frac{H_{\text{Linked}}}{H_{\text{TE alone}}}$  indicates the amount of hinge-moment reduction.)

The other flap configurations on the unswept wing give less hinge-moment reduction. For example, the addition of 0.05c leading-edge flaps to the unswept wing with 0.15c trailing-edge flaps (configuration .50.05.15 or .40.05.15) gives hinge-moment reductions of only about 0.2 at  $M = 1.414$  and 0.15 at  $M = 1.960$ . The reduction of hinge moment due to 0.05c leading-edge flaps thus compares more favorably with that due to 0.10c flaps at the lower Mach number than at the higher Mach number. This result occurs because the 0.05c flaps produce appreciably larger moment-relieving interference loads on the trailing-edge flap at the lower Mach number than at the higher Mach number. Primarily because of the large area moment of the 0.20c trailing-edge flap, the .50.10.20 configuration shows a larger percentage of unbalanced hinge moment than the .50.10.15 configuration. The two configurations with flaps of unequal span show small hinge-moment-reducing effectiveness.

On the  $45^\circ$  swept wing at  $M = 1.960$  the 0.10c leading-edge flap (configuration .50.10.15) leaves only about 0.2 of the hinge moment unbalanced (column 19), compared with 0.8 for the 0.05c flap (configuration .50.05.15). The large difference between the interference load due to the 0.10c and 0.05c flaps contributes to the large difference in balancing effectiveness.

The values of the parameter  $\frac{H}{2q\delta} \left(\frac{z}{b}\right)^3$  given in columns 3, 4, and 5 of table I are indicative of  $C_{h\delta}$ . For the unswept-wing combinations the values of  $\left[\left(\frac{H}{2q\delta}\right)\left(\frac{z}{b}\right)^3\right]_{\text{Linked}}$  decrease in magnitude with an increase in Mach number from 1.414 to 1.960, the greatest decrease being about 0.5 for the .50.10.15 configuration and the least decrease being about 0.3 for the .40.05.15 configuration. This decrease may be compared with a decrease of 0.4 for each of the trailing-edge flaps alone.

As  $M$  increases from 1.414 to 1.960, the percentage of hinge moment remaining unbalanced (column 19) becomes more for the .50.05.15 and .40.05.15 configurations, less for the .50.10.15 and .50.10.20 configurations, and is relatively constant for the .40.10.15 configuration. It may be seen that, for combinations with  $b_{f_{LE}} = b_{f_{TE}}$ , the configurations having 0.10c leading-edge flaps not only give the greater hinge-moment reductions  $\left(1 - \frac{H_{\text{Linked}}}{H_{\text{TE alone}}}\right)$  but also show the smaller percentage variation of this quantity with Mach number.

Unbalanced hinge moment required to produce unit rolling moment is indicated for the linked controls by the values of  $H/L'$  in column 18.

Compared on this basis the configurations employing 0.10c leading-edge flaps and 0.15c trailing-edge flaps require least hinge moment for unit rolling moment. Since addition of a leading-edge flap gives increased rolling moment (column 21 of table I) as well as decreased hinge moment (column 19), comparison of linked flaps with trailing-edge flaps alone on the basis of equal rolling moment is more favorable to the linked system than comparison on the basis of hinge moment only  $\left(\frac{H_{\text{Linked}}}{H_{\text{TE alone}}}\right)$ .

It may be noted that, for the equal rolling-moment comparison,

$\frac{(H/L')_{\text{Linked}}}{(H/L')_{\text{TE alone}}}$  may be obtained by dividing column 19 by column 21.

For leading- and trailing-edge flaps deflected singly, the hinge moments at  $M = 1.960$  can be obtained approximately from the values at  $M = 1.414$  by multiplying by the two-dimensional transformation factor  $\frac{\beta_{M=1.414}}{\beta_{M=1.960}} = \frac{1}{1.6857}$ . Hinge moments obtained in this way underestimate the correct values by less than 2.5 percent since the aspect ratios of the flaps are fairly large.

Deflection ratio for zero hinge moment with constant gearing ratio.-  
The deflection ratios necessary for the cancellation of all hinge moments with constant gearing ratio are given in column 22 of table I. These ratios reflect the trends of hinge-moment reducing effectiveness of leading-edge flaps shown by column 19 for  $\frac{\delta_{\text{LE}}}{\delta_{\text{TE}}} = 1$ . The 0.05c leading-edge-flap combinations on both swept and unswept wings require the larger deflection ratios. The short-span leading-edge flaps on the unswept wing also require large deflection ratios.

Variation with Mach number of the maximum deflection for which attached shock waves can be maintained (ref. 9) indicates that leading-edge angles must be less than  $9^\circ$  at  $M = 1.414$  and less than  $22^\circ$  at  $M = 1.960$ . Low deflection ratios are, therefore, mandatory if detached shock waves are to be avoided. Also, in application large leading-edge deflections would result in separation and the early occurrence of non-linear control characteristics. For total cancellation of hinge moments of 0.15c or 0.20c trailing-edge flaps, therefore, the use of at least a 0.10c leading-edge flap having the same span as the trailing-edge flap is strongly indicated.

Deflection ratio for zero hinge moment with nonconstant gearing ratio.- For the condition of zero hinge moment with nonconstant gearing

ratio, the necessary deflection ratios (column 23 of table I) are appreciably larger and show more variation with Mach number than do the values for the condition of constant gearing ratio. Therefore, the choice of a leading-edge flap for the reduction of hinge moment with nonconstant  $\frac{d\delta_{LE}}{d\delta_{TE}}$  appears to be more critical than for the reduction of hinge moment with constant  $\frac{d\delta_{LE}}{d\delta_{TE}}$ .

Effect of finite thickness.- The linearized-theory results have been corrected in accordance with appendix B for the effect of a 4-percent-thick symmetrical wedge airfoil section perpendicular to the 0.50c line with maximum thickness at the 0.50c line (columns 26 to 30 of table I). The effect of introducing finite wing thickness is to increase leading-edge-flap hinge moments and to decrease trailing-edge-flap hinge moments (see also ref. 10). For  $\delta_{LE} = \delta_{TE}$  the unbalanced hinge moments are reduced, the decrease in  $\frac{H_{linked}}{H_{TE \text{ alone}}}$  ranging from 4 percent to 20 percent for the unswept wing configurations. For  $\delta_{LE} = \delta_{TE}$  the .50.10.15 configuration on the swept wing becomes slightly overbalanced with the addition of thickness (column 26). The deflection ratios for  $H = 0$  with constant and nonconstant gearing ratio calculated from linearized theory are also reduced by the addition of thickness.

#### Lift and Rolling Moment

For  $\delta_{LE} = \delta_{TE}$  on the unswept wing the 0.40b/2 flap configurations show values of rolling moment per unit hinge moment  $L'/H$  which are slightly higher than the values for the corresponding 0.50b/2 configurations at both  $M = 1.414$  and  $M = 1.960$  (column 17 of table I). On the basis of lift per unit hinge moment  $L/H$ , there is little difference between values for corresponding 0.40b/2 and 0.50b/2 configurations at either Mach number (column 15). This latter result is also obtained for trailing-edge flaps alone (columns 14 and 16). The values of  $L'/H$  and  $L/H$  again reflect the superiority of 0.10c leading-edge flaps as compared with the 0.05c flaps. For either 0.05c or 0.10c leading-edge flaps the swept-wing combinations produce highest values of  $L'/H$  and  $L/H$ . The leading- and trailing-edge flap configurations of unequal span on the unswept wing yield low values of  $L'/H$  and  $L/H$ .

Lift and rolling moments per unit deflected area are indicated by  $C_{L,f\delta}$  and  $C_{l\delta} \frac{S}{S_f}$  values (columns 6 and 7 of table I). The deflection of

a leading-edge flap ( $\delta_{LE} = \delta_{TE}$ ) causes a loss in  $C_{L,f\delta}$  and  $C_{l\delta} \frac{S}{S_f}$ , the

loss becoming greater as the leading-edge-flap chord is increased. A comparison of values of  $C_{L,f\delta}$  for the .50.10.15 and the

.22, .50.10.15 configurations shows that the addition of the short-span leading-edge flap has a more detrimental effect on lift per unit area than the addition of the leading-edge flap having the same span as the trailing-edge flap. The swept-wing combinations give the highest  $C_{L,f\delta}$  values at  $M = 1.960$ .

For the leading- and trailing-edge flaps deflected singly, lift and rolling-moment coefficients at  $M = 1.960$  can be obtained approximately from the values at  $M = 1.414$  by multiplying by the two-dimensional transformation factor  $\frac{\beta_{M=1.414}}{\beta_{M=1.960}}$ . Values obtained in this way underestimate the correct values by less than 2.5 percent. Since this sort of variation has been indicated previously for hinge-moment coefficients, the values of  $L/H$  and  $L'/H$  for the trailing-edge flap alone change little with Mach number.

For  $\delta_{LE} = \delta_{TE}$ , application of the two-dimensional factor  $\frac{\beta_{M=1.414}}{\beta_{M=1.960}}$  results in underestimation of  $C_{L,f\delta}$  by 5 to 8 percent and underestimation of  $C_{l\delta} \frac{S}{S_f}$  by 8 to 13 percent. The smaller errors are obtained for combinations employing large-span and small-chord leading-edge flaps. Thus even though the two-dimensional factor would at best give only a rough approximation to the linked control  $C_{L,f\delta}$  and  $C_{l\delta} \frac{S}{S_f}$ , it does indicate that the addition of leading-edge flaps does not involve great changes in the variation of lift and rolling moment with Mach number.

Effect of finite thickness.- A comparison of columns 27 and 28 with columns 20 and 21 of table I indicates that including the effect of a 4-percent-thick wedge airfoil increases  $\frac{L_{\text{Linked}}}{L_{\text{TE alone}}}$  and  $\frac{L'_{\text{Linked}}}{L'_{\text{TE alone}}}$  by 3 to 7 percent for the leading- and trailing-edge flaps of equal span and by 2 to 3 percent for the flaps of unequal span.

## SUMMARY OF RESULTS

Linearized-theory analysis for a series of nine linked leading- and trailing-edge-flap combinations at Mach numbers of 1.414 and 1.960 and comparison of the results on the basis of equal deflection of leading- and trailing-edge flaps (except as noted) indicate the following:

1. For the cases of equal-span leading- and trailing-edge flaps, the addition of 0.10-chord leading-edge flaps to an unswept wing with 0.15-chord trailing-edge flaps at Mach numbers of 1.414 and 1.960 results in hinge-moment reductions of about 0.50. These hinge-moment reductions are accompanied by rolling moment increases of up to about 0.50.

2. For leading- and trailing-edge flaps of equal span, the addition of 0.05-chord leading-edge flaps to an unswept wing with 0.15-chord trailing-edge flaps results in hinge-moment reductions of about 0.2 at a Mach number of 1.414 and about 0.15 at a Mach number of 1.960.

3. Of the control combinations employing 0.10-chord leading-edge flaps the greatest hinge-moment reducing effectiveness is obtained on the  $45^\circ$  swept wing, and the least effectiveness is obtained on the unswept wing with leading-edge flaps of span shorter than that of the trailing-edge flap.

4. Hinge-moment reducing effectiveness for configurations with 0.4-semispan and 0.5-semispan flaps on the unswept wing are about the same at a Mach number of 1.414, but the 0.5-semispan combinations are somewhat more effective than the 0.4-semispan combinations at a Mach number of 1.960. In general, the configurations having 0.10-chord leading-edge flaps not only give the greater hinge-moment reductions but also show the smaller percentage variation of hinge-moment-reducing effectiveness with Mach number.

5. No great change in the effect of Mach number on lift and rolling moment is incurred by the addition of leading-edge flaps. For a given rolling moment the 0.4-semispan-flap configurations on the unswept wing give slightly greater hinge-moment reduction than 0.5-semispan configurations at Mach numbers of 1.414 and 1.960, but on the basis of a given lift the difference between them is small.

6. Since lift and rolling moment per unit deflected area are reduced somewhat by the presence of a leading-edge flap or by increasing its size, it follows that maintaining a desired lift or rolling moment while reducing hinge moment by means of a leading-edge flap requires an increase in the product of deflection angle and deflected area.

7. Comparison of the configurations on the basis of complete hinge-moment cancellation by use of a constant gearing ratio indicates that the 0.10-chord leading-edge flaps having span equal to trailing-edge flap span require smallest deflection ratios.

8. An approximate correction of the linearized-theory results for the effect of finite-wing thickness increases the calculated lift, rolling moment, and hinge moment for the leading-edge flap and reduces these quantities for the trailing-edge flap. Including the effect of a 4-percent-thick wedge airfoil gives ratios of linked-flap hinge moment to trailing-edge-flap-alone hinge moment which are lower than those obtained from linearized theory by as much as 19 percent.

Langley Aeronautical Laboratory,  
National Advisory Committee for Aeronautics,  
Langley Field, Va., November 8, 1955.

## APPENDIX A

## DETAILS OF THE LINEARIZED THEORY CALCULATIONS

The lift, rolling moment, and hinge moment caused by the deflections shown in figure 2 have been evaluated by superimposing the lift, rolling moment, and hinge moment caused by deflection of single "flaps." The superposition of these "flaps" used to obtain lift and rolling moment is shown in figure 3, and the superposition used to obtain interference hinge moment is shown in figure 4. Calculations of lift, rolling moment, and hinge moment for the individual "flaps" were based on the charts presented in reference 8, which were obtained from the linearized theory of two-dimensional and conical supersonic flows given in reference 7. Also, some unpublished equations obtained in connection with reference 8 have been used to adapt the results of that investigation for use in determining the interference loads. The charts of reference 8 presenting  $\beta C_{h\delta}$ ,  $\beta C_{L,f\delta}$ ,  $\beta C_{l,f\delta}$ ,  $\beta C_{m,HL\delta}$  (in the notation of the present report) for various combinations of the flap geometric parameters  $a$ ,  $d$ , and  $\lambda_f$  were used to evaluate these force and moment coefficients for the individual flaps. For present use  $\beta C_{h\delta}$ ,  $\beta C_{L,f\delta}$ ,  $\beta C_{l,f\delta}$ ,  $\beta C_{m,HL\delta}$  values for the original plots of reference 8 were plotted against the parameter  $a$  for the specific values of  $\lambda_f$  and  $d$  used in this analysis.

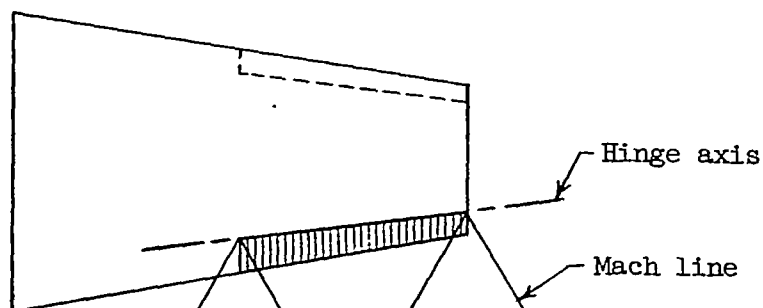
## Hinge Moment

The hinge moments of the leading-edge flap, the trailing-edge flap alone, and the interference load on the trailing-edge flap may be combined to give the total hinge moment of the system according to the equation

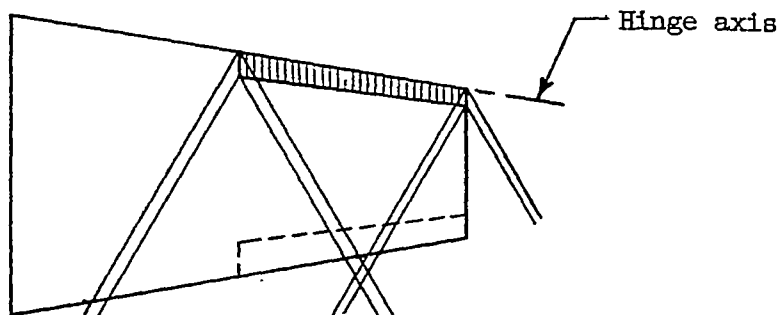
$$\frac{H}{2q\delta_{TE}} = \frac{H_{TE \text{ alone}}}{2q\delta_{TE}} + M_{a,TE} \Delta C_{h\delta} \frac{\delta_{LE}}{\delta_{TE}} + \frac{H_{LE}}{2q\delta_{LE}} \frac{d\delta_{LE}}{d\delta_{TE}} \frac{\delta_{LE}}{\delta_{TE}} \quad (A1)$$

Leading-edge and trailing-edge flaps deflected individually.- Values of lift, rolling-moment, and hinge-moment coefficients for trailing-edge

flap deflection alone (element C of fig. 3, shown below) were obtained directly from the coefficient plots.



Values of these coefficients for the leading-edge flap were also obtained directly from the plots by assuming the flap to be deflected about its leading edge, as indicated in the following sketch:

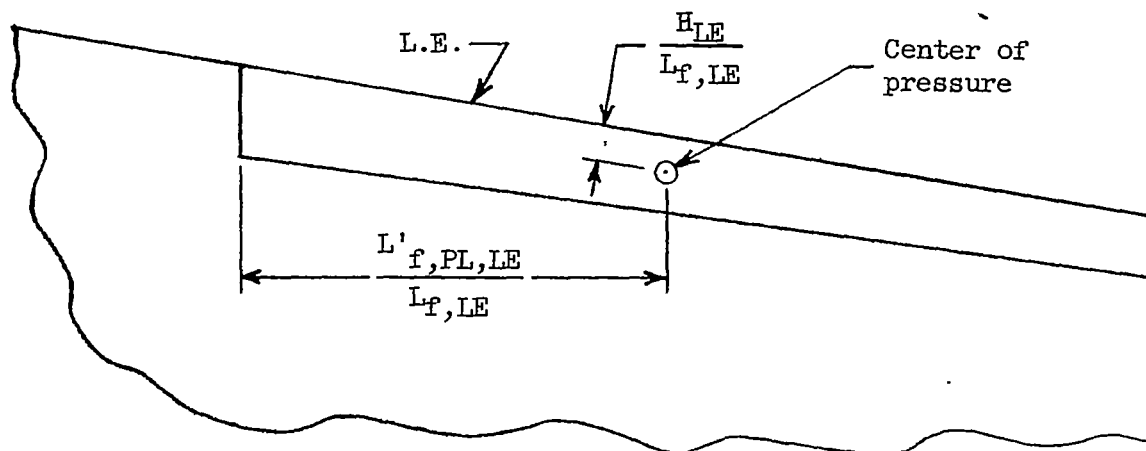


Errors resulting from this assumption were small because the leading edge and the hinge line of the leading-edge flap were very nearly parallel for the configurations investigated. The assumption was found to cause an error of less than 0.4 percent in the leading-edge-flap hinge moment. The aerodynamic coefficients  $C_{L,f\delta}$ ,  $C_{l,f\delta}$ , and  $C_{h\delta}$  were converted into lift ( $L/q\delta$ ), rolling moment ( $L'_{PL}/q\delta$ ), and hinge moment ( $H/2q\delta$ ) by multiplying each by the appropriate  $S_f$ ,  $b_f S_f$ , or  $M_a$ .

$$S_f = \frac{\beta b_f^2 (a - d) (1 + \lambda_f)}{2(1 - \lambda_f)} = \frac{1}{6} \frac{c_f}{c} \frac{b_f}{b/2} \left( \frac{1}{\lambda_f} + 1 \right) \left( \frac{b}{2} \right)^2 \quad (A2)$$

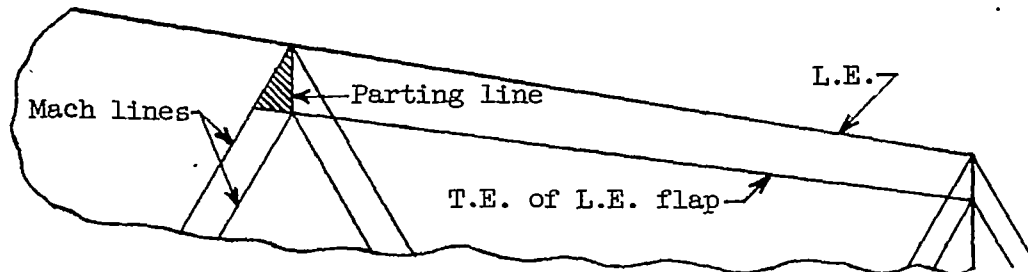
$$M_a = \frac{\beta^2 b_f^3 (a - d)^2 (1 - \lambda_f^3)}{6(1 - \lambda_f)^3 \sqrt{1 + \beta^2 a^2}} = \frac{1}{54} \left( \frac{c_f}{c} \right)^2 \frac{b_f}{b/2} \frac{1 + \lambda_f + \lambda_f^2}{\lambda_f^2} \frac{1}{\sqrt{1 + \beta^2 a^2}} \left( \frac{b}{2} \right)^3 \quad (A3)$$

The hinge line for the leading-edge flap was transferred to its trailing edge by a simple transfer of moments. For this transfer the flap center of pressure was located a distance of  $\frac{H(\text{about LE})}{L_{f,LE}}$  from the leading edge and a distance of  $\frac{L'_{f,PL,LE}}{L_{f,LE}}$  from the parting line.



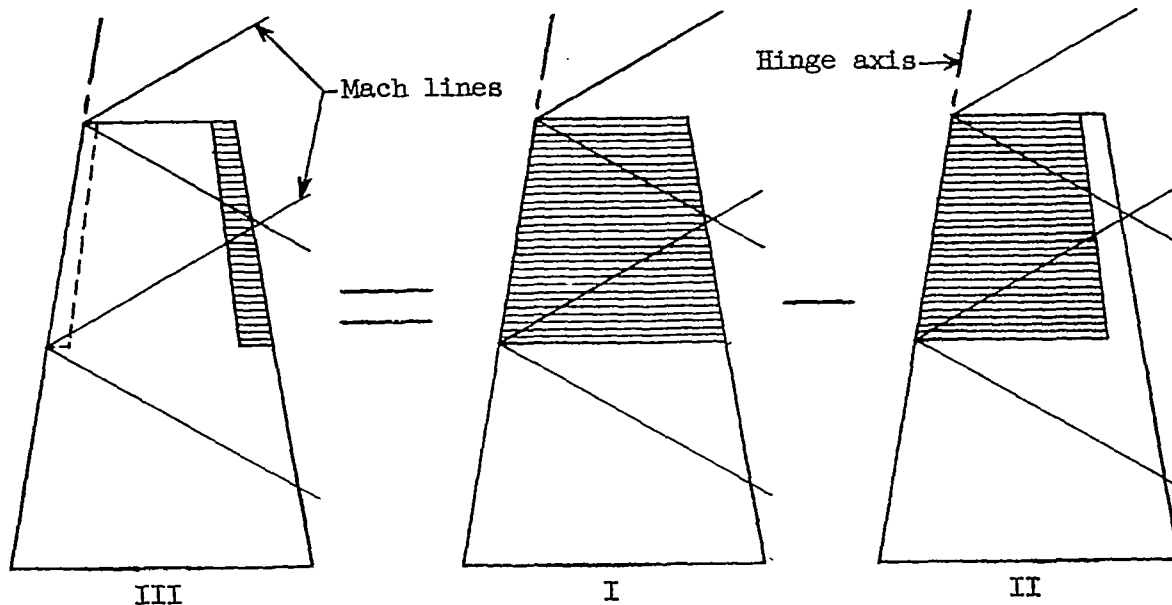
Since the lift and rolling moment computed from the coefficients of reference 8 include the "overflow" loading on the wing surface due to flap deflection, it was necessary to obtain  $L_f$  and  $L'_{f,PL}$  from  $L$  and  $L'_{PL}$  by subtracting out the lift and rolling moment contributed by the

triangular area just inboard of the flap and bounded by the parting line, the flap trailing edge extended, and the Mach line.

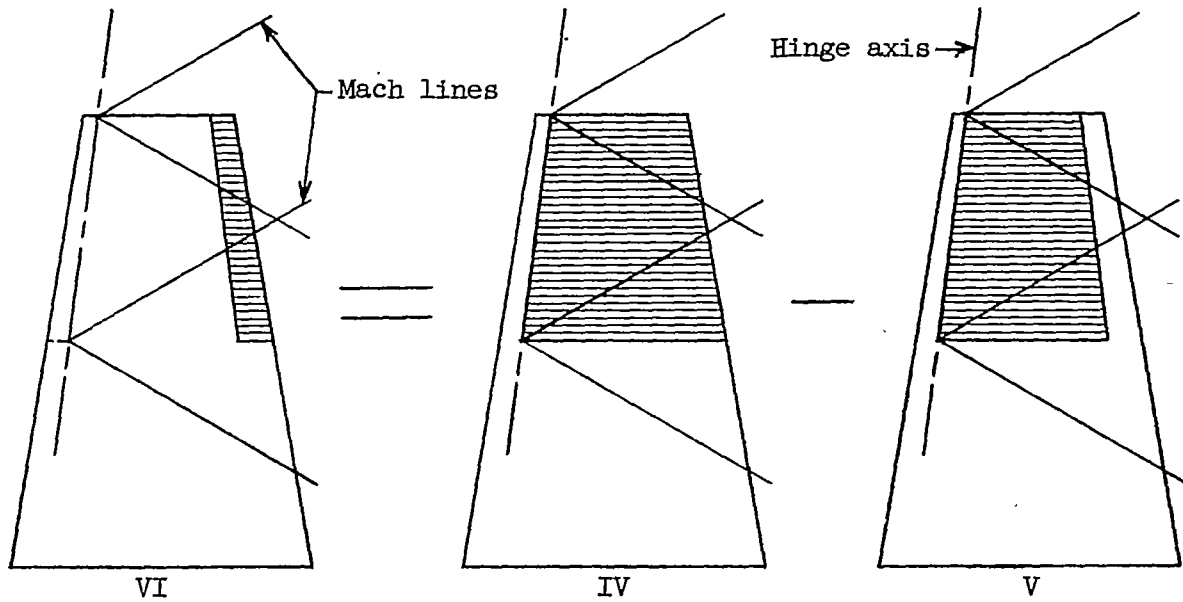


The lift and rolling moment for this area were obtained from the equations for average pressure ratio and center-of-pressure location given in table II of reference 8.

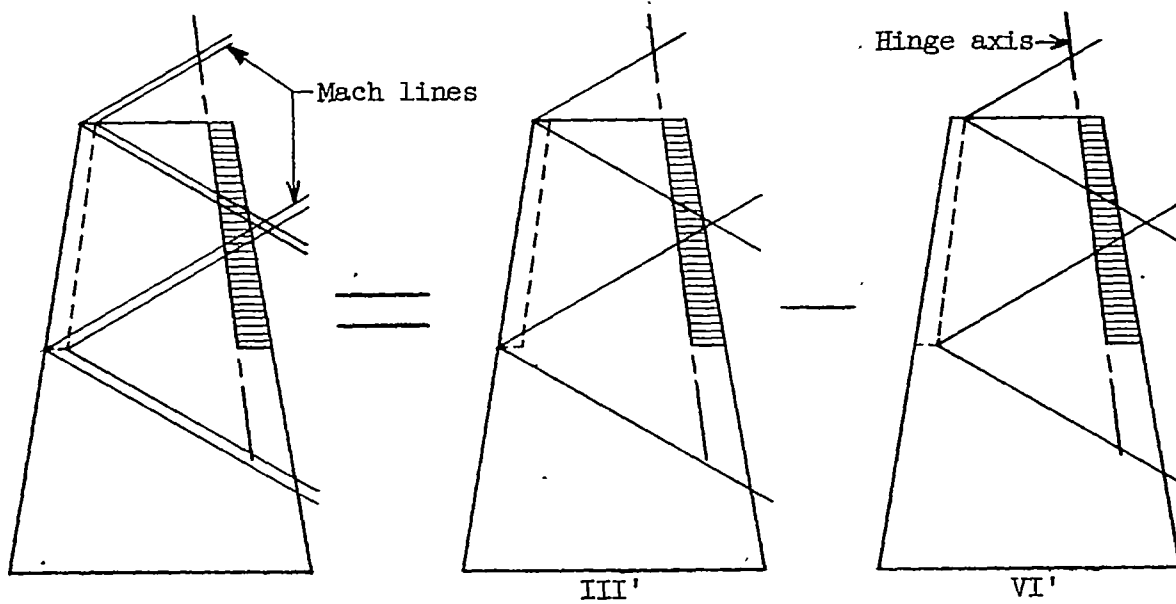
Trailing-edge-flap hinge moment due to interference from leading-edge flap for  $b_{f,LE} = b_{f,TE}$ .— The superposition of loadings used to obtain the hinge moment of the trailing-edge flap due to leading-edge flap deflection is shown for  $b_{f,LE} = b_{f,TE}$  in figure 4(a). The procedure consisted essentially in determining the loads and moments on the area occupied by the trailing-edge flap caused by deflection of that area about the wing leading edge (element III of fig. 4)



and by deflection about the leading-edge-flap hinge line (element VI of fig. 4)

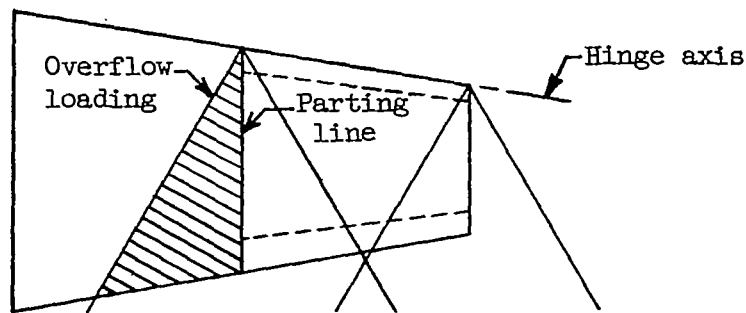


and then combining these to form the interference loads and moments on the trailing-edge flap.



Note that the hinge axes of elements III and VI have been transferred. The lift, rolling-moment, and hinge-moment coefficients for the

individual "flaps" (elements I, II, IV, V of fig. 4) were obtained from the plots of  $\beta C_{h\delta}$ ,  $\beta C_{L,f\delta}$ , and  $\beta C_{l,f\delta}$ , which were derived from reference 8 as described previously. Multiplication of the  $C_{L,f\delta}$ ,  $C_{l,f\delta}$ ,  $C_{h\delta}$  coefficients by  $S_f$ ,  $b_f S_f$ , and  $M_a$ , respectively, yielded lift, rolling moment, and hinge moment in the form  $L/q\delta$ ,  $L'_{PL}/q\delta$ ,  $H/2q\delta$ . In these calculations, as in the case of the leading-edge flap, it was necessary to alter the lift and rolling moments of elements I, II, IV, V (fig. 4(a)) by subtracting the lift and rolling moment contributed by the crosshatched triangular areas ("overflow" loading on the wing surface).



Thus, for example,

$$\frac{L_{f,I}}{q\delta} = \frac{L_I}{q\delta} - \frac{L_{\text{overflow}}}{q\delta}$$

and

$$\frac{L'_{f,PL,I}}{q\delta} = \frac{L'_{PL,I}}{q\delta} - \frac{L'_{PL,\text{overflow}}}{q\delta}$$

Then

$$\left. \begin{aligned} \frac{L_{f,III}}{q\delta} &= \frac{L_{f,I}}{q\delta} - \frac{L_{f,II}}{q\delta} \\ \frac{L_{f,VI}}{q\delta} &= \frac{L_{f,IV}}{q\delta} - \frac{L_{f,V}}{q\delta} \end{aligned} \right\} \quad (A4)$$

and

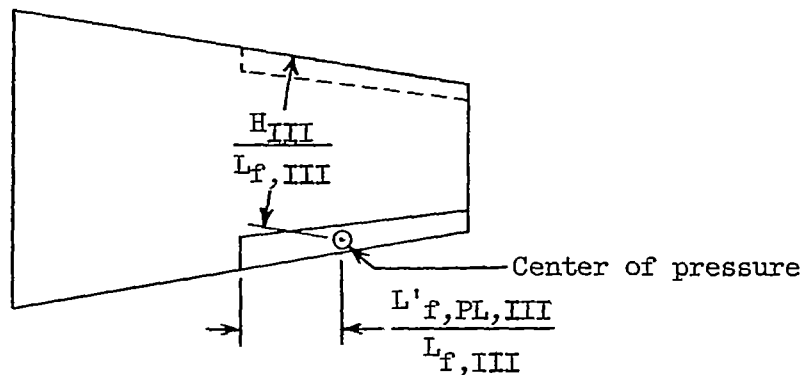
$$\left. \begin{aligned} \frac{L'_{f,PL,III}}{q\delta} &= \frac{L'_{f,PL,I}}{q\delta} - \frac{L'_{f,PL,II}}{q\delta} \\ \frac{L'_{f,PL,VI}}{q\delta} &= \frac{L'_{f,PL,IV}}{q\delta} - \frac{L'_{f,PL,V}}{q\delta} \end{aligned} \right\} \quad (A5)$$

The hinge moments were found directly from

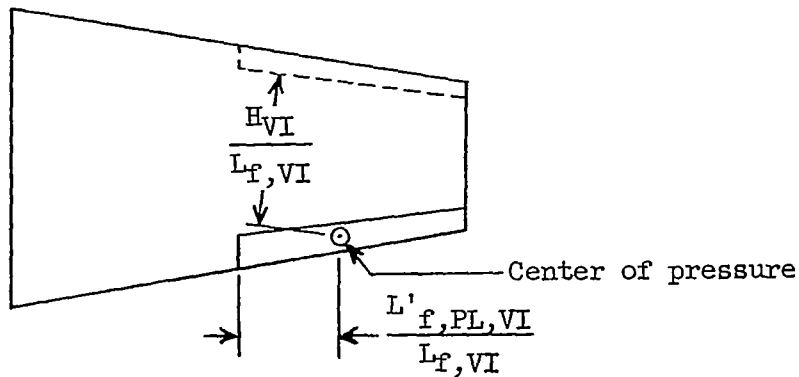
$$\left. \begin{aligned} \frac{H_{III}}{2q\delta} &= \frac{H_I}{2q\delta} - \frac{H_{II}}{2q\delta} \\ \frac{H_{VI}}{2q\delta} &= \frac{H_{IV}}{2q\delta} - \frac{H_V}{2q\delta} \end{aligned} \right\} \quad (A6)$$

The moment  $H_{III}$  is the moment of  $L_{f,III}$  about the wing leading edge, and  $H_{VI}$  is the moment of  $L_{f,VI}$  about the leading-edge-flap hinge line.

For the purpose of transferring the hinge axes to the hinge axis of the trailing-edge flap (from element III to III' and from element VI to VI' in figure 4(a)), the centers of pressure of the interference loads were located. For element III the center of pressure is  $\frac{H_{III}}{L_{f,III}}$  from the wing leading edge and  $\frac{L'_{f,PL,III}}{L_{f,III}}$  from the parting line.



For element VI the distances are  $\frac{H_{VI}}{L_{f,VI}}$  from the leading-edge-flap hinge line and  $\frac{L'_{f,PL,VI}}{L_{f,VI}}$  from the parting line.



From the geometry of the system these centers of pressure were located with respect to the trailing-edge-flap hinge line, and these distances were in turn multiplied by the appropriate  $L_{f,III}$  or  $L_{f,VI}$  to obtain

the interference contribution to trailing-edge-flap hinge moment. Thus,

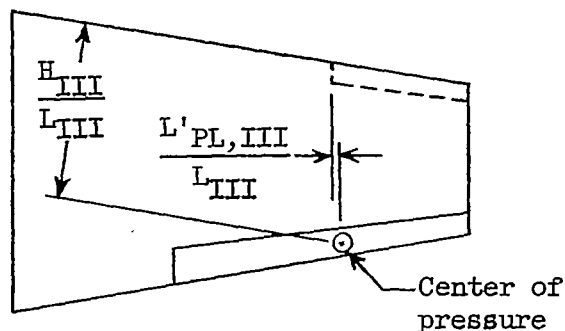
$$\Delta C_{h\delta} = \frac{H_{III}' - H_{VI}'}{2q\delta M_{a,TE}}$$

The subscript  $\delta$  refers to leading-edge-flap deflection.

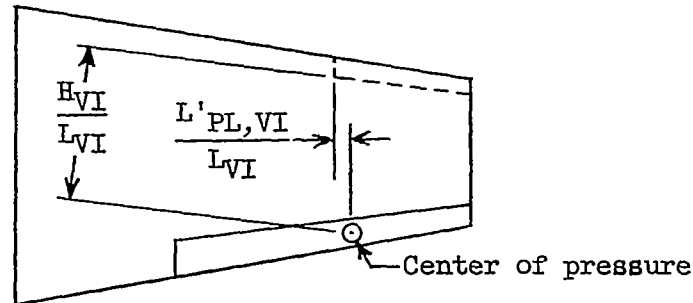
Trailing-edge-flap hinge moment due to interference from leading-edge flap for  $b_{f,LE} \neq b_{f,TE}$ . - For leading- and trailing-edge flaps of

unequal span the superposition procedure (fig. 4(b)) was similar to that for the flaps of equal span. However, the hinge moments  $H_{III}$  and  $H_{VI}$  caused by interference on the trailing-edge flap were found by combining the pitching moments (instead of the hinge moments) of elements I and II, and elements IV and V. In addition, for this case it was not necessary to correct for the lift and rolling moment contributed by the "overflow" loading on the wing surface (fig. 4(b)), since this loading is automatically accounted for. Thus, the center of pressure for element III is

$\frac{H_{III}}{L_{III}}$  from the wing leading edge and  $\frac{L'_{PL,III}}{L_{III}}$  from the parting line:



For the element VI the center of pressure is  $\frac{H_{VI}}{L_{VI}}$  from the leading-edge-flap hinge line and  $\frac{L'_{PL,VI}}{L_{VI}}$  from the parting line.



"Parting line" in this case refers to the parting line of elements I and II, and IV and V. The rest of the calculations were exactly the same as for  $b_{f,LE} = b_{f,TE}$ .

Deflection ratios.- The relative proportions in which the lifts, rolling moments, and hinge moments of leading-edge flap, trailing-edge flap alone, and interference on trailing-edge flap are combined depend on the deflection ratio  $\frac{\delta_{LE}}{\delta_{TE}}$  and gearing ratio  $\frac{d\delta_{LE}}{d\delta_{TE}}$ . For example, in general, the net hinge moment of the system as obtained from equation (A1) is

$$\begin{aligned}
 H &= H_{TE \text{ alone}} + 2qM_{a,TE} \Delta C_{h\delta} \delta_{LE} + H_{LE} \frac{d\delta_{LE}}{d\delta_{TE}} \\
 &= 2qM_{a,TE} C_{h\delta,TE \text{ alone}} \delta_{TE} + 2qM_{a,TE} \Delta C_{h\delta} \delta_{LE} + 2qM_{a,LE} C_{h\delta,LE} \delta_{LE} \frac{d\delta_{LE}}{d\delta_{TE}}
 \end{aligned}
 \tag{A7}$$

For the condition  $\frac{\delta_{LE}}{\delta_{TE}} = 1$ , this general equation reduces to (see column 5 of table I):

$$H = H_{TE \text{ linked}} + H_{LE} = 2qM_{a,TE} C_{h_{\delta,TE \text{ linked}}} \delta + H_{LE} = H_{\text{linked}} \quad (A8)$$

and

$$C_{h_{\delta,TE \text{ linked}}} = C_{h_{\delta,TE \text{ alone}}} + \Delta C_{h_{\delta}} \quad (A9)$$

If it is required that  $H = 0$  over a range of deflection, then  $\frac{\delta_{LE}}{\delta_{TE}}$  must be constant and equal to  $\frac{d\delta_{LE}}{d\delta_{TE}}$ , and the general equation for net hinge moment gives

$$\frac{\delta_{LE}}{\delta_{TE}} = -\frac{1}{2} \frac{M_{a,TE} \Delta C_{h_{\delta}}}{\left(\frac{H}{2q\delta}\right)_{LE}} + \frac{1}{2} \sqrt{\frac{(M_{a,TE} \Delta C_{h_{\delta}})^2}{\left(\frac{H}{2q\delta}\right)_{LE}^2} - 4 \frac{\left(\frac{H}{2q\delta}\right)_{TE \text{ alone}}}{\left(\frac{H}{2q\delta}\right)_{LE}}} \quad (A10)$$

Values of  $\frac{\delta_{LE}}{\delta_{TE}}$  computed from equation (A10) are given in column 22 of table I. It may be noted that this equation is also the condition for zero deflection work.

If it is required that  $H = 0$  and the gearing ratio  $\frac{d\delta_{LE}}{d\delta_{TE}}$  is not constant (and hence the deflection ratio  $\frac{\delta_{LE}}{\delta_{TE}}$  is not constant), the

general equation for net hinge moment gives

$$\frac{\delta_{LE}}{\delta_{TE}} = \frac{-\left(\frac{H}{2q\delta}\right)_{TE \text{ alone}}}{\left(\frac{H}{2q\delta}\right)_{LE} \left(\frac{d\delta_{LE}}{d\delta_{TE}}\right)_{H=0} + M_{a,TE} \Delta C_{h\delta}} \quad (A11)$$

or if  $\left(\frac{d\delta_{LE}}{d\delta_{TE}}\right)_{H=0}$  is arbitrarily taken to be unity, this equation becomes

$$\frac{\delta_{LE}}{\delta_{TE}} = \frac{1}{1 - \frac{H(\text{for } \delta_{LE} = \delta_{TE})}{H_{TE \text{ alone}}}} \quad (A12)$$

since

$$\left(\frac{H}{2q\delta}\right)_{\delta_{LE}=\delta_{TE}} = \left(\frac{H}{2q\delta}\right)_{TE \text{ alone}} + M_{a,TE} \Delta C_{h\delta} + \left(\frac{H}{2q\delta}\right)_{LE}$$

Values of  $\frac{\delta_{LE}}{\delta_{TE}}$  computed from equation (A12) are given in column 23 of table I.

#### Lift and Rolling Moment

Total lift and rolling moment are obtained by the superposition procedure shown in figure 3. Thus

$$\begin{aligned} \frac{L}{q\delta_{TE}} &= \frac{\delta_{LE}}{\delta_{TE}} \left[ \left( \frac{L}{q\delta} \right)_A - \left( \frac{L}{q\delta} \right)_B \right] + \left( \frac{L}{q\delta} \right)_C \\ &= \frac{\delta_{LE}}{\delta_{TE}} \left[ \left( C_{L,f\delta} S_f \right)_A - \left( C_{L,f\delta} S_f \right)_B \right] + \left( C_{L,f\delta} S_f \right)_C \end{aligned} \quad (A13)$$

and

$$\begin{aligned} \frac{L'}{q\delta_{TE}} &= \frac{\delta_{LE}}{\delta_{TE}} \left[ \left( \frac{L'}{q\delta} \right)_A - \left( \frac{L'}{q\delta} \right)_B \right] + \left( \frac{L'}{q\delta} \right)_C \\ &= \frac{\delta_{LE}}{\delta_{TE}} \left\{ \left( C_{L,f\delta} b_f S_f \right)_A - \left( C_{L,f\delta} b_f S_f \right)_B + \left[ \left( C_{L,f\delta} S_f \right)_A - \right. \right. \\ &\quad \left. \left. \left( C_{L,f\delta} S_f \right)_B \right] \left( \frac{b}{2} - b_f \right) \right\} + \left( C_{L,f\delta} b_f S_f \right)_C + \left( C_{L,f\delta} S_f \right)_C \left( \frac{b}{2} - b_f \right) \end{aligned} \quad (A14)$$

where subscripts A, B, C refer to the elements identified in figure 3. Element C is, of course, the trailing-edge flap alone.

Lift and rolling-moment coefficients presented in table I for the condition  $\delta_{LE} = \delta_{TE}$  were obtained from (columns 7 and 9 in table I):

$$C_{L,f\delta} = \frac{1}{S_{f,LE} + S_{f,TE}} \frac{L}{q\delta_{TE}}$$

$$C_{L\delta} = \frac{1}{S/2} \frac{L}{q\delta_{TE}}$$

and (columns 11 and 13 in table I):

$$C_{l\delta} \frac{S}{S_F} = \frac{l}{(S_{F,LE} + S_{F,TE})b/2} \frac{L'}{q\delta_{TE}}$$

$$C_{l\delta} = \frac{l}{Sb/2} \frac{L'}{q\delta_{TE}}$$

## APPENDIX B

## CORRECTION FOR FINITE THICKNESS

Estimation of the effect of finite thickness has been made by the method of reference 8. This method is based on the assumption that lift, rolling moment, and hinge moment may be corrected by considering

$$\frac{L, L', H(\text{3-dimensional, } t \neq 0)}{L, L', H(\text{3-dimensional, } t = 0)} = \frac{L, L', H(\text{2-dimensional, } t \neq 0)}{L, L', H(\text{2-dimensional, } t = 0)} = F_1, F_1, F_2$$

The correction should give most accurate results for surfaces over which the flow is largely two dimensional. Thus, the corrected results for hinge moment of the leading-edge flap and for lift, hinge moment, and rolling moment of the trailing-edge flap alone should be quite accurate. The accuracy obtained by applying this method to trailing-edge-flap hinge moment caused by leading-edge flap deflection and to the leading-edge-flap contribution to lift and rolling moment might be questionable. However, since these leading-edge-flap contributions form a relatively small portion of the total values, the correction is considered to give at least approximately correct overall values.

The correction factors  $F_1$  and  $F_2$  have been determined by using the Busemann second-order approximation to calculate  $L$  and  $H$  for two-dimensional sections with thickness. For symmetrical airfoil sections with trailing-edge flaps,

$$F_1 = \frac{1}{1 - \frac{x_{HL}}{c}} \int_{\frac{x_{HL}}{c}}^1 \left[ 1 + 2 \frac{c_2}{c_1} \frac{d\left(\frac{t}{2c}\right)}{d\left(\frac{x}{c}\right)} \right] d\left(\frac{x}{c}\right)$$

and

$$F_2 = \frac{2}{\left(1 - \frac{x_{HL}}{c}\right)^2} \int_{\frac{x_{HL}}{c}}^1 \left(\frac{x}{c} - \frac{x_{HL}}{c}\right) \left[1 + 2 \frac{C_2}{C_1} \frac{d\left(\frac{t}{2c}\right)}{d\left(\frac{x}{c}\right)}\right] d\left(\frac{x}{c}\right)$$

With leading-edge flaps,

$$F_1 = \frac{1}{\frac{x_{HL}}{c}} \int_0^{\frac{x_{HL}}{c}} \left[1 + 2 \frac{C_2}{C_1} \frac{d\left(\frac{t}{2c}\right)}{d\left(\frac{x}{c}\right)}\right] d\left(\frac{x}{c}\right)$$

and

$$F_2 = \frac{2}{\left(\frac{x_{HL}}{c}\right)^2} \int_0^{\frac{x_{HL}}{c}} \left(\frac{x_{HL}}{c} - \frac{x}{c}\right) \left[1 + 2 \frac{C_2}{C_1} \frac{d\left(\frac{t}{2c}\right)}{d\left(\frac{x}{c}\right)}\right] d\left(\frac{x}{c}\right)$$

In these equations,  $\frac{d\left(\frac{t}{2c}\right)}{d\left(\frac{x}{c}\right)}$  is the slope of the airfoil section in the

direction perpendicular to the hinge line (for trailing-edge flaps) or perpendicular to the leading edge (for leading-edge flaps). The factors  $C_1$  and  $C_2$  are functions only of the component of  $M$  in the

direction of  $\frac{d\left(\frac{t}{2c}\right)}{d\left(\frac{x}{c}\right)}$ . Values of  $C_1$  and  $C_2$  are given in table IV of reference 11.

Values of  $F_1$  and  $F_2$  (columns 24 and 25 of table I) have been calculated for a 4-percent-thick symmetrical wedge airfoil section perpendicular to the  $0.50c$  line with  $(t/c)_{\max}$  at the  $0.50c$  line. The

values of  $\frac{H_{\delta, LE=\delta, TE}}{H_{TE \text{ alone}}}$ ,  $\frac{L_{\delta, LE=\delta, TE}}{L_{TE \text{ alone}}}$ , and  $\frac{L'_{\delta, LE=\delta, TE}}{L'_{TE \text{ alone}}}$  for equal deflection

of leading- and trailing-edge flaps,  $\frac{\delta_{LE}}{\delta_{TE}}$  for zero hinge moment were cal-

culated from the equations used above for the zero-thickness calculation. For wings with finite thickness, however, each term in the equations for  $L$ ,  $L'$ , and  $H$  was multiplied by the appropriate  $F_{LE}$  or  $F_{TE}$ . For example, for  $\delta_{LE} = \delta_{TE}$ ,

$$\left( C_{h_{\delta, TE \text{ linked}}} \right)_{t \neq 0} = F_{2, TE} \left( C_{h_{\delta, TE \text{ alone}}} \right)_{t=0} + F_{2, LE} \left( \Delta C_{h_{\delta}} \right)_{t=0}$$

The finite-thickness results are presented in columns 26 to 30 of table I.

It should be noted that, in general, thickness corrections for loadings caused by disturbances originating from the leading-edge-flap hinge line are different from those for loadings caused by disturbances originating at the leading edge. If the leading-edge-flap hinge line is not parallel to the leading edge, the normal component of  $M$  is different for these two lines. Except for flat-sided airfoils, the surface slopes are different at leading-edge and leading-edge-flap hinge line. For configurations used in the present analysis, however, it has been assumed that the same correction factors apply for leading-edge disturbances and for leading-edge-flap hinge-line disturbances, since this assumption results in less than 0.05 percent error in the final ratios (columns 26 to 30 of table I).

## REFERENCES

1. Goin, Kenneth L.: Theoretical Analyses To Determine Unbalanced Trailing-Edge Controls Having Minimum Hinge Moments Due to Deflection at Supersonic Speeds. NACA TN 3471, 1955. (Supersedes NACA RM L51F19.)
2. Kuhle, E.: A Tail Unit With Leading Edge Flap as an Elevator Balancer. TPA3/TIB Translation No. GDC. 10/288. T., British Ministry of Supply, 1942.
3. White, Roland J.: A New Method of Longitudinal Control for Aircraft by Use of an Adjustable Angle of Attack Balance. Jour. Aero. Sci., vol. 10, no. 5, May 1943, pp. 152-160.
4. Conner, D. William, and Mitchell, Meade H., Jr.: Control Effectiveness and Hinge-Moment Measurements at a Mach Number of 1.9 of a Nose-Flap and Trailing-Edge Flap on a Highly Tapered Low-Aspect-Ratio Wing. NACA RM L8K17a, 1949.
5. Boatright, William B., and Rainey, Robert W.: Hinge-Moment Measurements of a Wing With Leading-Edge and Trailing-Edge Flaps at a Mach Number of 1.93. NACA RM L8K12a, 1949.
6. Strass, H. Kurt: Free-Flight Investigation of the Rolling Effectiveness at High Subsonic, Transonic, and Supersonic Speeds of Leading-Edge and Trailing-Edge Ailerons in Conjunction With Tapered and Untapered Plan Forms. NACA RM L8E10, 1948.
7. Lagerstrom, P. A., and Graham, Martha E.: Linearized Theory of Supersonic Control Surfaces. Jour. Aero. Sci., vol. 16, no. 1, Jan. 1949, pp. 31-34.
8. Goin, Kenneth L.: Equations and Charts for the Rapid Estimation of Hinge-Moment and Effectiveness Parameters for Trailing-Edge Controls Having Leading and Trailing Edges Swept Ahead of the Mach Lines. NACA Rep. 1041, 1951. (Supersedes NACA TN 2221.)
9. Ivey, H. Reese, Stickle, George W., and Schuettler, Alberta: Charts for Determining the Characteristics of Sharp-Nose Airfoils in Two-Dimensional Flow at Supersonic Speeds. NACA TN 1143, 1947.
10. Morrisette, Robert R., and Oborny, Lester F.: Theoretical Characteristics of Two-Dimensional Supersonic Control Surfaces. NACA TN 2486, 1951. (Supersedes NACA RM L8G12.)
11. The Staff of the Ames 1- by 3-Foot Supersonic Wind-Tunnel Section: Notes and Tables for Use in the Analysis of Supersonic Flow. NACA TN 1428, 1947.

TABLE I.- CHARACTERISTICS OF TRAILING-EDGE FLAPS DEFLECTED SIMPLY

AND IN COMBINATION WITH LEADING-EDGE FLAPS

[All values are for  $\delta_{LE} = \delta_{TE}$  except those in columns 22, 23, 29, and 30](a) Linearized Theory Results;  $A = 4$ ;  $\lambda = 0.5$ 

1	2	3	4	5	6	7	8	9	10	11	12	13
Flap configuration (a)	$C_{H_0}$ T.E. alone	$\frac{H(\frac{a}{b})^3}{2qb}$ T.E. alone	$\frac{H(\frac{a}{b})^3}{2qb}$ L.E. alone	$\frac{H(\frac{a}{b})^3}{2qb}$ Linked	$C_{L,f_0}$ T.E. alone	$C_{L,f_0}$ Linked	$C_{L_0}$ T.E. alone	$C_{L_0}$ Linked	$C_{L_0} \frac{a}{b}$ T.E. alone	$C_{L_0} \frac{a}{b}$ Linked	$C_{L_0}$ T.E. alone	$C_{L_0}$ Linked
$\Lambda_c/2 = 0$ ; $M = 1.414$												
.50.05.15	-0.03350	$-0.3293 \times 10^{-4}$	$0.0384 \times 10^{-4}$	$-0.2519 \times 10^{-4}$	0.07542	0.06861	0.004714	0.005718	0.05298	0.04579	0.001655	0.001906
.50.10.15	-.03350	-.5293	.1520	-.1832	.07542	.06483	.004714	.006756	.05298	.04176	.001655	.002173
.40.05.15	-.03333	-.2406	.0281	-.1860	.07490	.06650	.003595	.004256	.05701	.04810	.001569	.001540
.40.10.15	-.03333	-.2406	.1111	-.1335	.07490	.06185	.003595	.004948	.05701	.04518	.001569	.001727
.50.10.20	-.03273	-.5730	.1520	-.4168	.07313	.06506	.006094	.008136	.05148	.04263	.002144	.002664
$\Lambda_c/2 = 0$ ; $M = 1.960$												
.50.05.15	-0.02025	$-0.1990 \times 10^{-4}$	$0.0226 \times 10^{-4}$	$-0.1720 \times 10^{-4}$	0.04549	0.04280	0.002843	0.003564	0.03204	0.02959	0.001001	0.001232
.50.10.15	-.02025	-.1990	.0398	-.0892	.04549	.04120	.002843	.004294	.03204	.02821	.001001	.001470
.40.05.15	-.02018	-.1457	.0164	-.1351	.04537	.04188	.002178	.002680	.03470	.03145	.000853	.001006
.40.10.15	-.02018	-.1457	.0651	-.0829	.04537	.03993	.002178	.003194	.03470	.02967	.000853	.001186
.50.10.20	-.01994	-.3491	.0698	-.2360	.04351	.04060	.003626	.005076	.03092	.02812	.001269	.001758
.22,.50.10.15	-.02025	-.1990	.0295	-.1635	.04549	.04099	.002843	.003228	.03204	.02907	.001001	.001145
.30,.65.10.15	-.02029	-.2933	.0439	-.2449	.04560	.04209	.003928	.004590	.02795	.02653	.001204	.001448
$\Lambda_0/4 = 45^\circ$ ; $M = 1.960$												
.50.05.15	-0.02102	$-0.1624 \times 10^{-4}$	$0.0517 \times 10^{-4}$	$-0.1307 \times 10^{-4}$	0.05695	0.04919	0.003559	0.004098	0.03968	0.03439	0.001240	0.001433
.50.10.15	-.02102	-.1624	.1226	-.0264	.05695	.04507	.003559	.004696	.03968	.03148	.001240	.001640

<sup>a</sup>In the three-number designations the first numeral denotes  $\frac{b_f}{b/2}$  for both leading and trailing-edge flap; the second,  $\frac{c_{f,LE}}{c}$ ; the third  $\frac{c_{f,TE}}{c}$ .  
In four-number designation, the first numeral denotes  $\frac{b_{f,LE}}{b/2}$  and the second,  $\frac{b_{f,TE}}{b/2}$ .

TABLE I.- CHARACTERISTICS OF TRAILING-EDGE FLAPS DEFLECTED SINGLY

AND IN COMBINATION WITH LEADING-EDGE FLAPS - Continued

[All values are for  $\delta_{LE} = \delta_{TE}$  except those in columns 22, 23, 29, and 30]

(a) Linearized Theory Results;  $A = 4$ ;  $\lambda = 0.5$  - Concluded

1 (repeated)	14	15	16	17	18	19	20	21	22	23
Flap configuration (a)	$\frac{L}{H}$ T.E. alone	$\frac{L}{H}$ Linked	$\frac{L'}{H}$ T.E. alone	$\frac{L'}{H}$ Linked	$\frac{H}{L'}$ Linked	$\frac{H_{Linked}}{H_{TE} \text{ alone}}$	$\frac{L_{Linked}}{L_{TE} \text{ alone}}$	$\frac{L'_{Linked}}{L'_{TE} \text{ alone}}$	$\frac{\delta_{LE}}{\delta_{TE}}$ H = 0 for $\frac{d\delta_{LE}}{d\delta_{TE}} = \text{Const}$	$\frac{\delta_{LE}}{\delta_{TE}}$ H = 0 for $\frac{d\delta_{LE}}{d\delta_{TE}} \neq \text{Const}$
$\Lambda_0/2 = 0; M = 1.414$										
.50.05.15	-35.8	-36.8	-25.1	-37.9	-0.0264	0.765	1.214	1.152	2.46	4.25
.50.10.15	-35.8	-92.2	-25.1	-59.3	-.0169	.556	1.433	1.315	1.49	2.26
.40.05.15	-37.4	-37.2	-28.5	-41.4	-.0242	.773	1.184	1.125	2.49	4.42
.40.10.15	-37.4	-92.7	-28.5	-64.7	-.0155	.555	1.376	1.262	1.49	2.25
.50.10.20	-26.6	-48.8	-18.7	-32.0	-.0313	.727	1.335	1.242	1.93	3.67
$\Lambda_c/2 = 0; M = 1.960$										
.50.05.15	-35.7	-51.8	-25.2	-33.8	-0.0279	0.864	1.254	1.230	2.87	7.36
.50.10.15	-35.7	-100.3	-25.2	-72.5	-.0121	.448	1.509	1.468	1.38	1.81
.40.05.15	-37.3	-50.3	-28.6	-37.8	-.0263	.914	1.231	1.209	3.10	11.61
.40.10.15	-37.3	-96.4	-28.6	-72.6	-.0140	.569	1.468	1.425	1.51	2.32
.50.10.20	-26.0	-53.3	-18.5	-37.0	-.0270	.682	1.400	1.365	1.86	3.14
.22,.50.10.15	-35.7	-49.4	-25.2	-33.0	-.0286	.822	1.135	1.144	2.50	5.59
.30,.65.10.15	-33.5	-46.9	-20.5	-29.6	-.0338	.835	1.169	1.203	2.54	6.07
$\Lambda_0/4 = 45^\circ; M = 1.960$										
.50.05.15	-54.8	-78.4	-38.2	-54.9	-0.0182	0.805	1.151	1.155	2.26	5.13
.50.10.15	-54.8	-444.7	-38.2	-310.7	-.0032	.163	1.319	1.322	1.10	1.19

<sup>a</sup>In three-number designations the first numeral denotes  $\frac{b_f}{b/2}$ ; the second,  $\frac{c_{f,LE}}{c}$ ; the third  $\frac{c_{f,TE}}{c}$ .

In four-number designations, the first numeral denotes  $\frac{b_{f,LE}}{b/2}$  and the second  $\frac{b_{f,TE}}{b/2}$ .

TABLE I.- CHARACTERISTICS OF TRAILING-EDGE FLAPS DEFLECTED SINGLY

AND IN COMBINATION WITH LEADING-EDGE FLAPS - Concluded

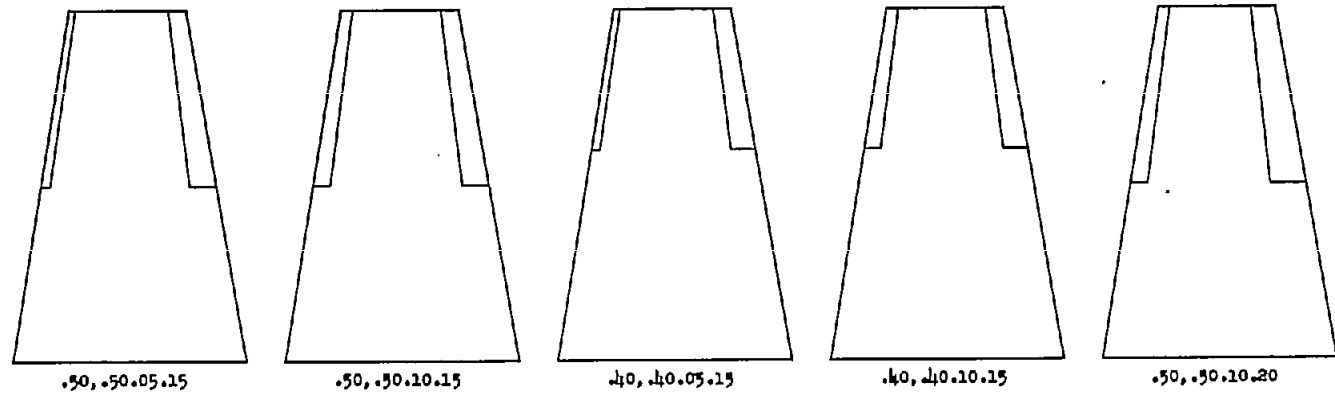
[All values are for  $\delta_{LE} = \delta_{TE}$  except those in columns 22, 23, 29, and 30]

(b) Linearized Theory Results Corrected for a 4-percent-Thick

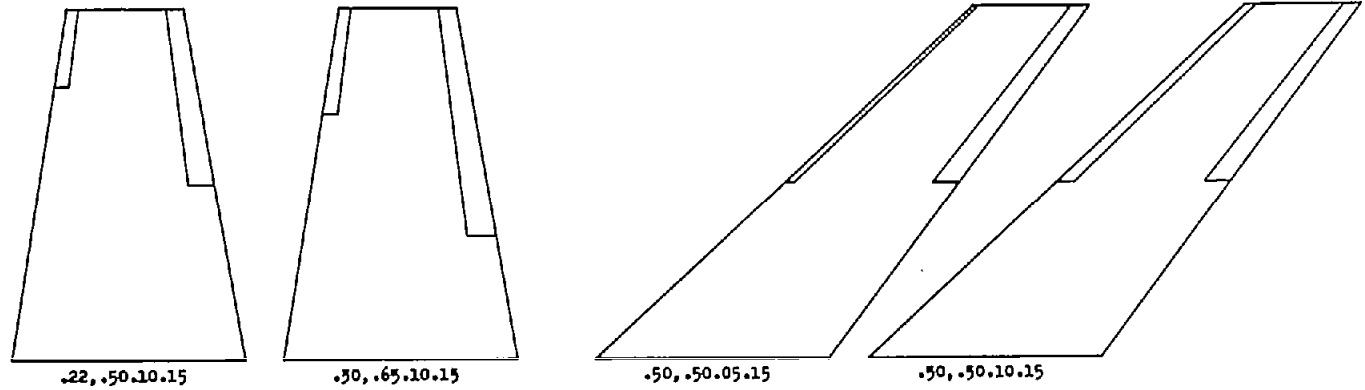
Symmetrical Wedge Airfoil;  $A = 4$ ;  $\lambda = 0.5$

1 (repeated)	24	25	26	27	28	29	30
Flap configuration (a)	$F_1 = F_2$ L.E.	$F_1 = F_2$ T.E.	$\frac{H_{\text{linked}}}{H_{TE} \text{ alone}}$	$\frac{L_{\text{linked}}}{L_{TE} \text{ alone}}$	$\frac{L'_{\text{linked}}}{L'_{TE} \text{ alone}}$	$\frac{\delta_{LE}}{\delta_{TE}}$ H = 0 for $\frac{d\delta_{LE}}{d\delta_{TE}} = \text{Const}$	$\frac{\delta_{LE}}{\delta_{TE}}$ H = 0 for $\frac{d\delta_{LE}}{d\delta_{TE}} \neq \text{Const}$
$\Lambda_c/2 = 0; M = 1.414$							
.50.05.15	1.1123	0.8922	0.707	1.266	1.190	2.16	3.41
.50.10.15	1.1123	.8922	.448	1.540	1.392	1.34	1.81
.40.05.15	1.1123	.8922	.718	1.230	1.156	2.19	3.54
.40.10.15	1.1123	.8922	.446	1.470	1.326	1.34	1.80
.50.10.20	1.1123	.8959	.659	1.420	1.302	1.72	2.94
$\Lambda_c/2 = 0; M = 1.960$							
.50.05.15	1.0971	0.9052	0.835	1.307	1.280	2.60	6.07
.50.10.15	1.0971	.9052	.330	1.618	1.568	1.25	1.49
.40.05.15	1.0971	.9052	.879	1.280	1.252	2.85	9.58
.40.10.15	1.0971	.9052	.478	1.566	1.515	1.38	1.91
.50.10.20	1.0971	.9039	.613	1.486	1.442	1.68	2.59
.22,.50.10.15	1.0971	.9052	.785	1.164	1.167	2.26	4.61
.30,.65.10.15	1.0971	.9052	.800	1.203	1.233	2.30	5.01
$\Lambda_c/4 = 45^\circ; M = 1.960$							
.50.05.15	1.1329	0.9095	0.775	1.188	1.194	2.05	4.45
.50.10.15	1.1329	.9095	-.046	1.397	1.401	.98	.96

<sup>a</sup>In three-number designations used the first numeral denotes  $\frac{b_f}{b/2}$ ; the second,  $\frac{c_{f,LE}}{c}$ ; the third,  $\frac{c_{f,TE}}{c}$ . In four-number designations, the first numeral denotes  $\frac{b_{f,LE}}{b/2}$  and the second  $\frac{b_{f,TE}}{b/2}$ .



(a)  $b_{f,LE} = b_{f,TE}$ ;  $\Lambda_c/2 = 0$ ;  $\lambda = 0.5$ ;  $A = 4$ .



(b)  $b_{f,LE} \neq b_{f,TE}$ ;  $\Lambda_c/2 = 0$ ;  $\lambda = 0.5$ ;  
 $A = 4$ .

(c)  $b_{f,LE} = b_{f,TE}$ ;  $\Lambda_c/4 = 45^\circ$ ;  $\lambda = 0.5$ ;  
 $A = 4$ .

Figure 1.- Leading- and trailing-edge flap configurations. (Numbers under each wing indicate  $\frac{b_{f,LE}}{b/2}$ ,  $\frac{b_{f,TE}}{b/2}$ ,  $\frac{c_{f,LE}}{c}$ ,  $\frac{c_{f,TE}}{c}$ .)

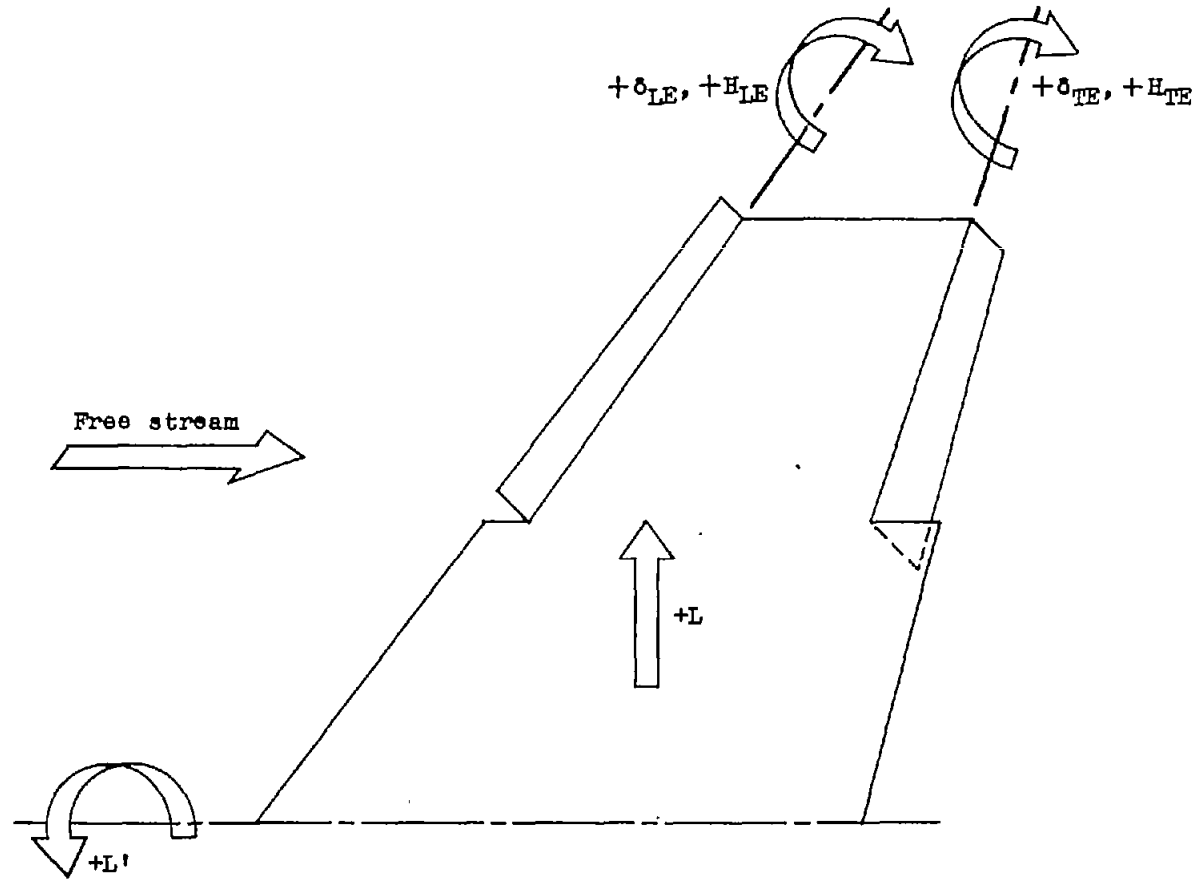


Figure 2.- Signs and directions of force, moment, and deflection.

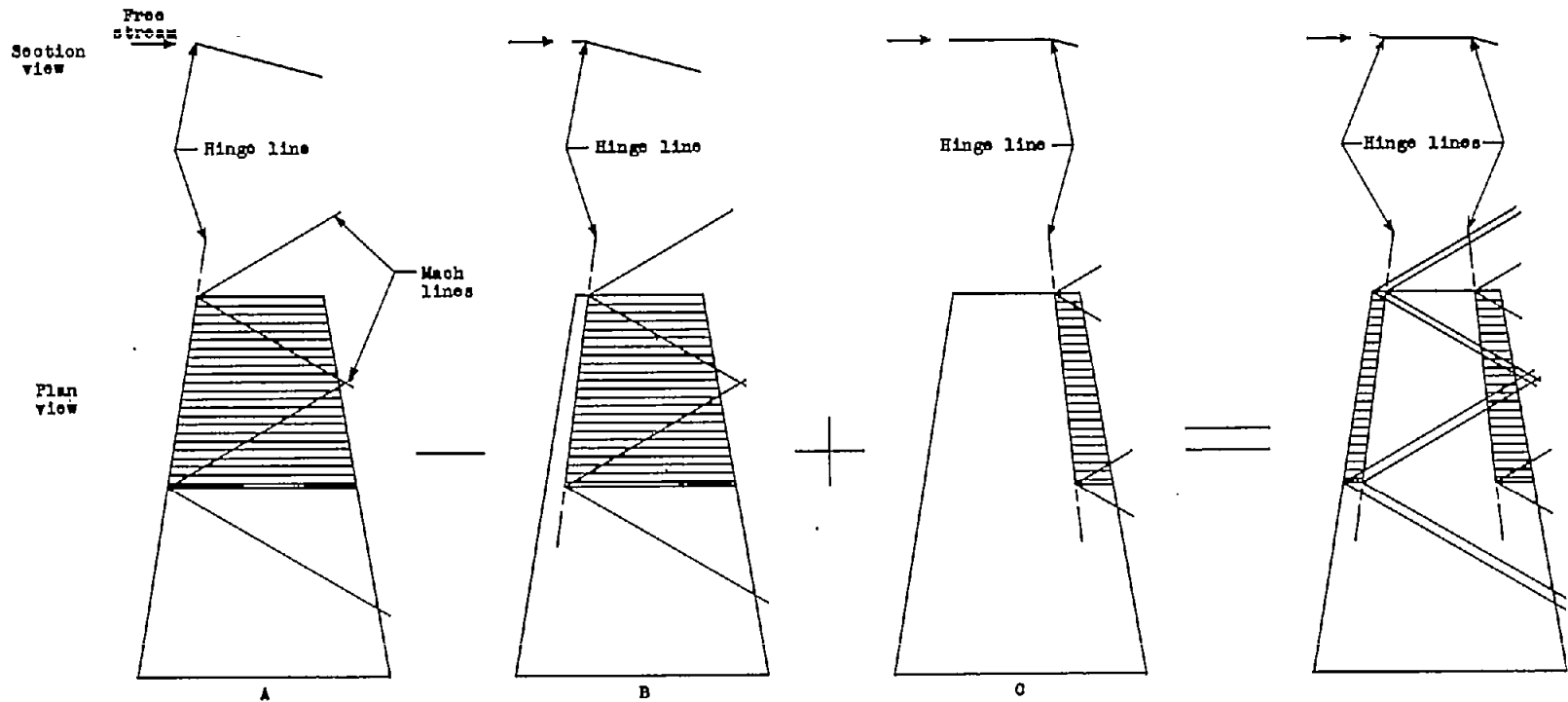
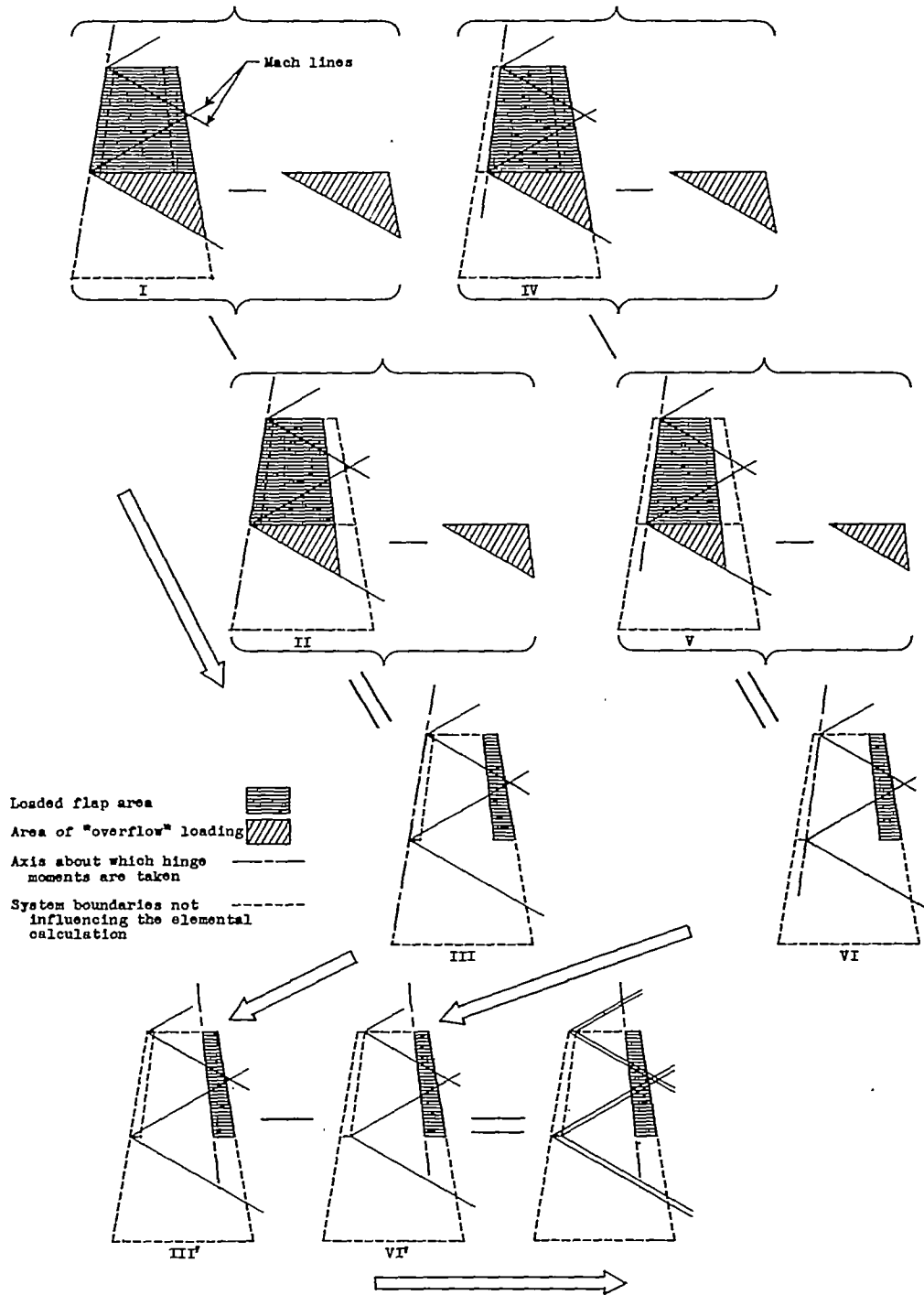
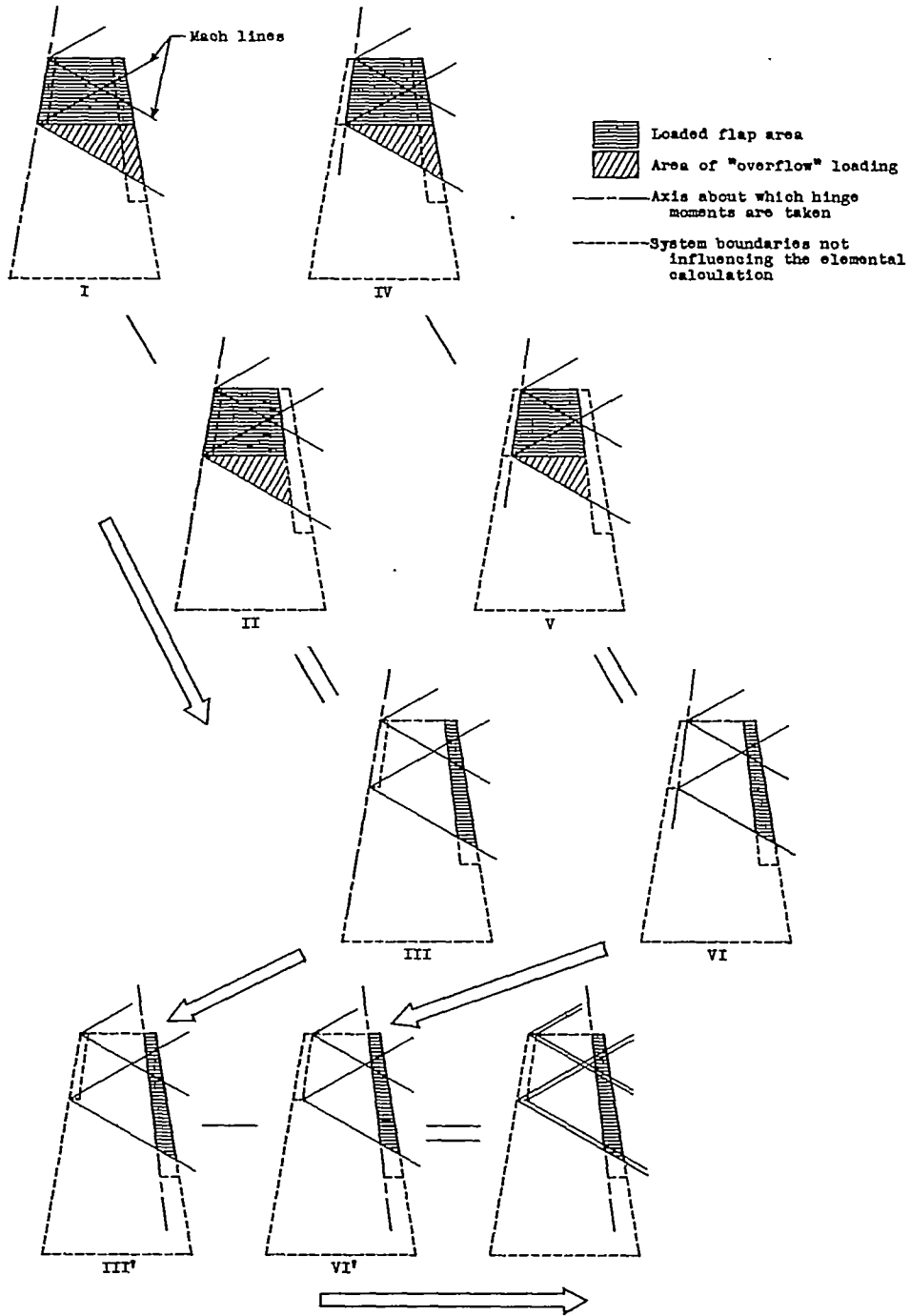


Figure 3.- Superposition procedure used to obtain simultaneous deflection of leading- and trailing-edge flaps.



(a)  $b_{f,LE} = b_{f,TE}$ .

Figure 4.- Combination of loadings used to obtain  $\Delta C_{hs}$ . (See appendix A for details.)



(b)  $b_{f,LE} \neq b_{f,TE}$